Advances in Science and Technology Research Journal

Advances in Science and Technology Research Journal, 2026, 20(7), 210–226
https://doi.org/10.12913/22998624/219079
ISSN 2299-8624, License CC-BY 4.0

Received: 2026.01.05
Accepted: 2026.05.15
Published: 2026.06.01

Web-post buckling resistance prediction models of stainless-steel cellular beams using machine learning algorithms

Imane Bachguar[1], Ouadia Mouhat[1*], Rabee Shamass[2], Ikram Abarkan[3]

[1] Mohammed V University, Mohammadia Engineering School, Civil Engineering and Environment Laboratory (LGCE), Rabat, Morocco
[2] Department of Civil and Environmental Engineering, Brunel University London, London, UK
[3] Department of Physics, Faculty of Sciences, Abdelmalek Essaadi ˆ University, 93002, Tetouan, Morocco
* Corresponding author's e-mail: ouadia.mouhat@gmail.com

ABSTRACT

Cellular steel beams are increasingly used in construction projects due to their decorative and economical characteristics, enabling long spans that reduce the number of columns and footings in the structure, thus shortening construction times and reducing infrastructure costs. The objective of this paper is to prognosticate the ultimate strength, and to realize an accurate design method for determining the web-post buckling of stainless-steel cellular beams using machine learning. Several machine learning algorithms are trained using dataset generated from validated finite element models (FEM), including artificial neural networks, decision trees and random forests. All these models performed remarkably well, with coefficients of determination R^2 greater than 0.9. The artificial neural network stood out for its superior predictive capacity, offering the best results. In particular, the ANN model with 8 neurons produced very accurate predictions for estimating the web-post buckling strength. In conclusion, a formula based on artificial neural networks (ANN) was presented and proved to be highly accurate, with a regression value (R^2) equal to 0.99823, and mean absolute error (MAE), root mean square error (RMSE) values equal to 11.19 and 17.29 respectively. The formula based on artificial neural networks can therefore be used as a design tool.

Keywords: artificial neural networks, cellular beams, stainless steel, buckling, FEM.

INTRODUCTION

Cellular steel beams are gaining popularity in construction for their aesthetic, economic, and technical advantages. Cellular beams offer a high degree of flexibility during construction, saving both time and space [1], because their openings allow mechanical, electrical, and plumbing services to pass through the beam, eliminating the need for additional space below for these installations. This integration optimizes floor-to-ceiling heights and reduces structural depth. Cellular beams are frequently used in composite floor systems, the aim being to design and produce beams with long spans [2]. These Cellular beams are manufactured either by cutting sections of rolled steel lengthways, then re-welding the two parts together to create a deeper beam with circular holes, or by welding the plates together to form the beam, in a similar way to a plate girder. This method allows the dimensions of the flange and web to be adapted to suit the load, the shape of the construction and the opening requirements [3]. These beams are highly efficient because they combine enhanced flexural strength with reduced material self-weight [2]. The geometric parameters of the formed cellular beam are shown in Figures 1 and 2.

However, the presence of these openings strongly affects the strength of the beams, as it causes a change in their behavior and stability. They become highly susceptible to several modes of buckling, namely: web-post buckling, lateral-torsional buckling, Vierendeel mechanism or even sometimes the beam may suffer a combination of different failure modes. The complexity of

these phenomena has been extensively studied. For instance, Ellobody [4] conducted a non-linear finite element analysis to study and analyze the interaction of several buckling modes in cellular steel beams. In order to examine the inelastic behavior of cellular beams and subsequently identify and determine moment gradient factors that improve the prediction of flexural capacity, El-Sawy et al. [5] created a 3D non-linear finite element model. Subsequently, Ferreira et al. [6] studied the lateral-torsional buckling behavior of cellular beams and assessed its implications for the evolution of the Eurocode 3 design rules.

Several experimental studies have been carried out on cellular steel beams to determine and analyze their structural behavior and define their failure modes [7–8]. As a result, the literature currently contains numerous studies dealing with the various failure modes encountered in cellular steel beams. Grilo et al [7] suggested a new design procedure based essentially on resistance curves, which makes it possible to determine the shear resistance of steel cellular beams in the case of web-post buckling. In addition, Panedpojaman et al. [8] conducted an in-depth numerical study and proposed new design equations for the shear resistance of local web-post buckling, taking into account the effect of geometric parameters.

Shamass and Guarracino [9] presented a robust design approach to anticipate the web-post buckling in normal and high-strength steel cellular beams. This method makes it possible to determine the parameters that influence the onset and evolution of web-post buckling, for both normal and high-strength steels. In their paper, Shamass et al [10] propose an artificial neural network (ANN) model that can reliably predict web-post buckling resistance and identify the failure mode of steel beams with elliptical openings. The conclusion of the study is that the five-neural model can accurately predict the buckling resistance of the web column. Ellobody [4] used a variety of buckling modes as a reference to analyze the nonlinear behaviour of normal and high-strength steel beams. The main objective was to define the impact of steel strength, beam length, geometric variations in cross-section and non-dimensional slenderness ratio on the failure loads of cellular steel beams. Lawson et al. [11] proposed a simplified approach to assess the web-post buckling. This method takes into account the asymmetry of the cross-section and is based mainly on a strut model. Carvalho et al. [12] conducted a study analyzing the stability of beams with sinusoidal openings using three types of stainless steel: austenitic stainless steel, high-strength stainless steel S600E, and ferritic stainless steel. An artificial neural network model was developed based on 9,720 finite element models, and a computer program was created to facilitate the use of the trained model. Sharifi et al. [13] proposed a formula developed using an artificial neural network based on 96 validated simulations. The goal is to reliably predict the ultimate load of steel cellular beams subjected to lateral-torsional buckling. Sharifi et al. [14] developed a reliable neural network to train a new formula capable of accurately estimating the ultimate load of cellular beams subjected to lateral-torsional buckling (LTB). After evaluating the performance of nine different learning algorithms, they concluded that the Levenberg–Marquardt algorithm provided the most accurate results, with a low mean squared error. Limbachiya and Shamass [15] developed a formula using an artificial neural network capable of accurately determining the web-post buckling resistance. To this end, 16 artificial neural networks were trained, then tested and validated against 304 finite element models. Other studies carried out on different systems, such as the inelastic buckling of columns [16] or the degradation of bracing systems under cyclic loading [17], highlight the importance of extending analyses to sensitivity to imperfections and behavior under repeated loads.

The choice of a material for a specific application implies the need to guarantee its durability, particularly in the context of its environment of use, especially when it comes to systems exposed to corrosive atmospheres. Corrosion resistance plays a vital role in preserving the durability of steel structures, hence the strong interest in stainless steels. In addition to their excellent mechanical properties, such as hardness, impact strength and inherent corrosion resistance, stainless steel structural elements are characterized by complex behavior under extreme conditions. These conditions have been studied in specialized contexts, such as the fire resistance of stainless steel I-beams subject to lateral-torsional buckling [18] or the load-bearing capacity of welded sections made of high-strength stainless steel [19]. This resistance is due to the formation of a protective layer on the surface, mainly composed of iron and chromium oxides and hydroxides. Stainless steel is widely used today in many buildings and structural applications, thanks to its physical, mechanical and above all chemical properties. Its predominant

characteristic lies in its exceptional corrosion resistance, as well as a high hardening capability and elevated ductility [20]. Austenitic steel is the type of stainless steel most commonly used in this type of application, due to its optimal performance.

Machine learning is currently considered to be the most powerful branch of artificial intelligence. It is widely used in many professional fields, including science, medicine, engineering, construction, architecture and the automotive industry [21]. This field offers a particular opportunity to improve the predictability of structural engineering because of its ability to manage and deal with complex, non-linear structural systems. The researchers chose the machine learning approach to evaluate the performance of steel structures because it teaches computer systems to define correlations and relationships between input and output data so that the necessary predictions can be made. In addition, it allows computer systems to learn on their own and become more competent. Adeli and Yeh [22] were among the first to apply machine learning to structural engineering in 1989. One of the first applications of this technology in this field was the design of steel beams using an artificial neural network. Typically, each machine learning model uses multiple data sets to first model and then solve problems using computer-aided machines [7]. Once the data has been collected and analysed, machine learning algorithms are able to make decisions based on previous experience, leading to the most accurate solutions. To this end, it is essential to choose the characteristics of the data associated with the problem wisely, ensuring that there are enough of them. This allows the machine learning algorithms to solve the problem efficiently.

As of now, no research is being conducted to predict web-post buckling of stainless steel cellular beams using machine learning. Machine learning enables fast and accurate prediction of stainless steel cellular beam capacity by capturing complex nonlinear behavior and geometric interactions better than traditional methods. It reduces reliance on time-consuming FEA and supports real-time design optimisation. Among the machine the available learning models, there are ANNs, the Decision Tree and the Random Forest algorithm. The main aim of this study is to accurately predict the ultimate strength and develop a reliable design method for evaluating the web-post buckling of stainless steel cellular beams, and then to develop an equation for accurately calculating the web-post buckling resistance as a function of independent geometric parameters. To this end, finite element-based models were developed using ABAQUS software and then subjected to validation by comparison with previous experimental results, which were obtained by Grilo et al. [7]. The combination of experimental and numerical approaches to validate models is a widely recognized practice, as demonstrated by studies carried out on non-traditional structural materials, particularly HDPE turbine runners [23].It is important to note that these experimental studies are generally carried out on cellular carbon steel beams. In the literature, there are no tests that specifically address and examine the behavior of stainless steel cellular beams, so we proceeded to use these data to validate our numerical model. It is widely accepted that the stress-strain behavior of stainless steel differs from that of carbon steel, but the purpose of this validation step is to determine the model's ability to reproduce the failure mode and buckling kinematics of the web, which are mainly governed by geometry and elastic stability.

Based on previous research, the following hypotheses are formulated and tested during this study. First, it will be demonstrated that artificial neural networks (ANN) offer superior accuracy and generalization capabilities compared to Random Forest and Decision Tree machine learning models, enabling them to be used to develop an appropriate sizing formula. Subsequently, the methodology based on a combination of finite element simulations and machine learning is an effective solution for providing design rules for stainless steel cellular beams, even in the absence of an experimental database.

DEVELOPMENT AND VALIDATION OF THE NUMERICAL MODELS

The choice and selection of our finite element model is a crucial and very important step in accurately predicting the behavior of cellular beams. To this end, this study was based on the finite element model previously developed by Shamass and Guarracino [9] using ABAQUS software. This model was found to be effective in providing accurate predictions of the behavior of cellular steel beams, particularly with respect to vertical shear resistance and failure of the beam web. These researchers used simply supported

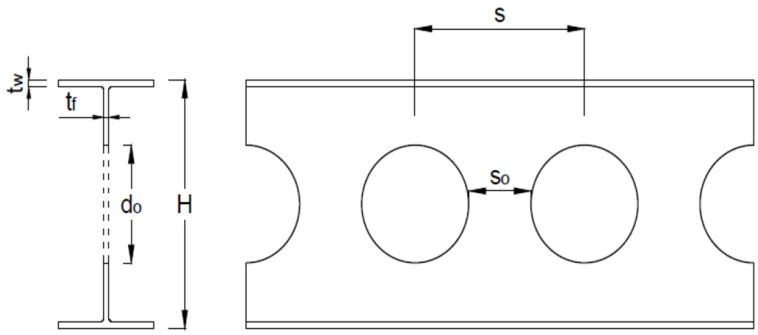

Figure 1. Cellular beam geometry

cellular beams subjected to point loading in their experiments. To validate these finite element models, the results of tests previously carried out by Grilo et al. [7] and Tsavdaridis and D'Mello [24] were used. It is important to note that these experimental studies were mainly carried out on carbon steel cellular beams. However, due to the absence of tests specifically dedicated to the behaviour of stainless steel cellular beams in the literature, these data were used to validate our numerical model.

All numerical simulations undertaken to assess the capacity of beams to resist lateral bending are performed using ABAQUS software. These simulations encompass a complete set of 1000 beam models using the finite element method.

Each numerical model follows a two-stage process: the first is the elastic stage, which deals with the buckling phenomenon. This analysis takes no imperfections into account, and enables critical buckling loads to be determined and calculated for each structure. The second is the inelastic stage, which deals with post-buckling. Unlike the elastic analysis, for the inelastic analysis an initial geometric imperfection of H/500 is taken into consideration [8]. The geometric imperfection H/500 was chosen because it represents a realistic manufacturing tolerance. This value is used in several established numerical models for analyzing the buckling of cellular beams [15]. The imperfection value H/500 was generalized for all parametric models in order to ensure internal consistency within the training database.

In order to determine and validate the most appropriate model for our parametric study on the prediction of buckling shear load of WPB, Table 1 compares the experimental results (V_{Test}) obtained by Grilo et al [7] and Tsavdaridis and D'Mello [24] with the numerical results (V_{FE}) obtained using two models: the single web column model and the full beam model. The results indicate that the single web column model generally produces more conservative estimates than the full beam model.

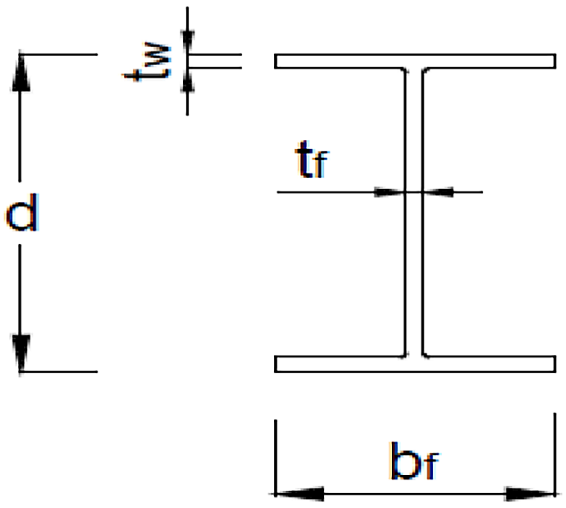

Figure 2. Parent I-beam section

PARAMETRIC STUDY

In order to carry out our parametric study, a single web-post model is used to determine the web-post buckling of stainless steel cellular beams. Using a single web-post instead of the complete specimen will enable us to study the web-post buckling phenomenon accurately, without the influence of other phenomena, namely the stiffening phenomenon caused mainly by the beam edges.

The parameters that define the web-beam geometries resulting from the cutting of the rolled I-beam are as follows [25].

$$e = \frac{d_0}{2} - \sqrt{\left(\frac{d_0}{2}\right)^2 - \left(\frac{s - d_0}{2}\right)^2} \qquad (1)$$

Table 1. Comparison between experimental and numerical vertical shear buckling load

Specimen	Buckling shear strength (V) (kN)			Percentage of difference (%)	
	Test (V_{test})	Numerical model (V_{FE})			
		Full beam	Single web-post	Full beam/test	Single web-post/test
A1	38	45.17	43.02	18.9	13.2
A2	61.9	60.6	63.85	-2.1	3.2
A3	70.7	64.63	73.85	-8.6	4.5
A5	99.1	104.74	92.13	5.7	-7.03
A6	102.2	102.25	116.7	0.05	14.2
B1	54	64.79	58.25	20	7.9
B2	79	68.83	81.24	-12.9	2.8
B5	138.5	149.14	129.47	7.7	-6.5
B6	150	145.72	158.01	-2.9	5.3

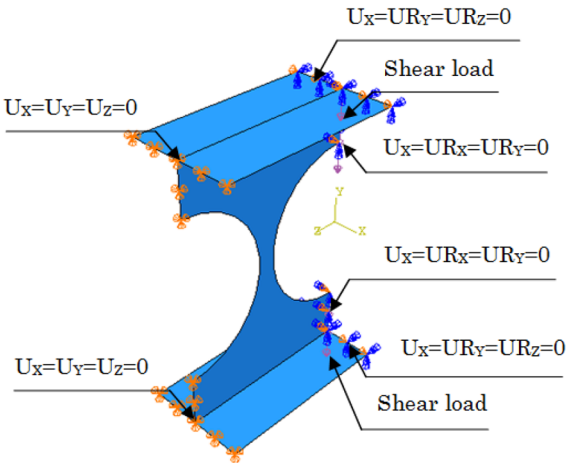

Figure 3. Geometrical configuration of single web-post and the considered boundary conditions

$$H = d + \frac{d_0}{2} - e \tag{2}$$

$$s_0 = s - d_0 \tag{3}$$

where: s_0 – the web-post width, H – the cellular beam height; d – the parent section height, H – the cellular beam height.

To carry out this study, finite element models were validated, then a parametric study was carried out by modifying the spacing, opening and slenderness ratios (s/d_0, d_0/d and d/t_w) respectively(d_0 – the opening height (Figure 3).

- The ratio s/d_0 is between 1.1 and 1.4 with a margin of 0.1;
- The ratio d_0/d is between 0.8 and 1.2 with a margin of 0.1;
- The d/t_w ratio corresponds to the data presented in the following Table 2.

To ensure that the distribution of geometric variables was uniform, the parametric space was sampled using a well-structured approach. The values of s/d_0, d_0/d and d/t_w were systematically discretized in order to generate combinations that avoided excessive concentration in certain regions of the parametric domain. Before proceeding with training, the database was examined to ensure that there was no imbalance or concentration of samples. The data was then randomly shuffled and divided into subgroups for training, validation and testing in order to reduce any potential bias. The observed concordance between the neural network predictions and the EF results shows that machine learning models have good generalization capabilities and are not influenced by the database structure.

It is important to note that predictions are only reliable for input values within these ranges.

Table 2. The I-beam sections used in this study

Section UB	152 × 89 × 16	203 × 133 × 25	254 × 102 × 28
d/t_w	33.87	35.65	41.33
Section UB	254 × 146 × 43	305 × 127 × 48	305 × 165 × 54
d/t_w	36.06	34.56	39.29

Therefore, any extrapolation outside this range may lead to unreliable results.

MATERIALS

The primary focus of the study will be on Austenitic stainless steel grades 1.4301, 1.4435, and 1.4541. The behavior of stainless steel differs from that of carbon steel. Whereas carbon steel is characterized by a clearly defined yield strength and low strain hardening, stainless steel exhibits a more curvilinear behavior with no clearly defined flow stress. Consequently, "yield strength" values for stainless steels are generally expressed in terms of a conventional yield strength established for a strain of 0.2%.

The two-stage stress-strain relationship developed by Rasmussen [26]. Clearly describes the material model used in numerical modeling:

$$\varepsilon = \frac{\sigma}{E} + 0.002\left(\frac{\sigma}{\sigma_{0.2}}\right)^{n} \quad \text{for } 0 \le \sigma \le \sigma_{0.2} \tag{4}$$

$$\varepsilon = \varepsilon_{0.2} + \frac{\sigma - \sigma_{0.2}}{E_2} + \varepsilon_{up}^{*}\left(\frac{\sigma - \sigma_{0.2}}{\sigma_u - \sigma_{0.2}}\right)^{m}$$

$$\text{for } \sigma_{0.2} \le \sigma \le \sigma_u \tag{5}$$

where:

$$\varepsilon_{up}^{*} = \varepsilon_u - \varepsilon_{0.2} - \frac{\sigma_u - \sigma_{0.2}}{E_2}$$

$$m = 1 + 3.5\frac{\sigma_{0.2}}{\sigma_u}$$

$$\varepsilon_u = \min\left(1 - \frac{\sigma_{0.2}}{\sigma_u}, A\right)$$

$$E_2 = \frac{E}{1 + 0.002n/e}$$

$$e = \frac{\sigma_{0.2}}{E}$$

where: ε_u – the ultimate tensile strain, A – the stainless steel elongation, m and n – strain hardening coefficients, E – the modulus of elasticity; $\mathcal{E}$ and σ – the uniaxial strain and stress.

Five different grades of stainless steel were selected for the parametric study. Table 3 shows the material properties of the steels used.

ARTIFICIAL NEURAL NETWORK

Neural network architecture

The artificial neural network is a machine learning model that is widely used to predict the structural behavior of various steel elements. These include cellular or crenellated steel beams [27–28], I-beams [29] and frames [30]. This artificial neural network (ANN) represents a computational structure composed of multiple processing units. Each unit receives input data and generates an output based on a predetermined activation function. Using MATLAB's neural network toolbox, this paper uses a neural network architecture, specifically a multilayer perceptron (MLPN) [31]. Data from our parametric study were exploited through the application of a two-layer feed-forward neural network. The data were divided into three sets: training 70%, validation 15% and test 15%. The activation

Table 3. Mechanical properties of stainless steels used for the parametric study

Specimen	Buckling shear strength (V) (KN)			Percentage of difference (%)	
	Test (V_{test})	Numerical model (V_{FE})			
		Full beam	Single web-post	Full beam/test	Single web-post/test
A1	38	45.17	43.02	18.9	13.2
A2	61.9	60.6	63.85	-2.1	3.2
A3	70.7	64.63	73.85	-8.6	4.5
A5	99.1	104.74	92.13	5.7	-7.03
A6	102.2	102.25	116.7	0.05	14.2
B1	54	64.79	58.25	20	7.9
B2	79	68.83	81.24	-12.9	2.8
B5	138.5	149.14	129.47	7.7	-6.5
B6	150	145.72	158.01	-2.9	5.3

functions for the hidden layer and output layer were determined as TANSIG (Equation 6) and PURELIN (Equation 7), respectively.

$$y = tansig(x) = \frac{2}{1+e^{-2x}} - 1 \tag{6}$$

$$y = purlin(x) = x \tag{7}$$

In this study, we opted for the Levenberg-Marquardt backpropagation training algorithm, due to its high accuracy, which has been demonstrated in previous studies [32–33]. In general, this algorithm requires less time and fewer iterations to reach convergence. Its superior performance compared to other learning methods makes it an optimal choice for training various networks.

The construction of the ANN model involves several essential parameters, such as the input elements, the number of neurons present in the hidden layer, the choice of activation function and finally the output parameters. Using this artificial neural network we will be able to predict the buckling resistance of stainless steel cellular beams based on the set of input parameters detailed below. The web-post buckling depends mainly on the geometry of the beam and the mechanical properties of the chosen material. Hence, the choice of input parameters has been divided into two categories. The first represents the geometric category, which is expressed in the parameters H, d_o, s and t_w (the web thickness). The second contains the mechanical parameters ε_{up}, n and E_2 (the slope of the stress-strain curve at $\varepsilon_{0.2}$ – the 0.2% strain corresponding to $\sigma_{0.2}$), which directly influence the way in which the steel deforms, and therefore have a direct effect on the resistance to shear buckling. Our goal is to study the effect of geometric and mechanical parameters on buckling, which is why the choice of input parameters focused on all parameters that directly influence the strength of the beam. A preliminary sensitivity analysis was carried out to verify and analyze the relevance of the selected input parameters. This confirms their physical importance and justifies their inclusion in the input data set.

The number of neurons in the hidden layer is an important factor in determining the accuracy of the ANN model (Figure 4). In this study, we developed and tested various ANN models, adjusting both the number of hidden layers and the number of neurons in them, as shown in Tables 3 and 5. Equations 8 and 9 describe the calculations involving the transfer function required to obtain the normalized output value as a function of the input data provided [34].

$$O_S = B_1^S + \sum_{k=1}^{r} \left(\omega_{k,1}^{h_0} \frac{2}{1+e^{-2H_k}} - 1\right) \tag{8}$$

$$H_k = B_2^k + \sum_{j=1}^{q} \omega_{j,k}^{ih} . I_j \tag{9}$$

where: q represents the number of input parameters; O_s is the normalized output value; r denotes the number of hidden neurons; s is the number of output parameters; B_1^s and B_2^k are the biases of sth output neuron and kth hidden neuron (H_k), respectively; $w^{ih}_{j,k}$ represents the weights of the connection between I_j and H_k; $w^{ho}_{k,l}$ are the weights of the connection between H_k and O_s.

To avoid the problem of overfitting, we divided our data into three sets (70% training, 15% validation and 15% testing) in order to evaluate and test the network's generalization capacity. Otherwise, we would not know whether our network had actually acquired the relationship between the input and output parameters. The validation set allows the model's performance to be examined throughout the training phase. In addition, for each iteration, the training and validation errors were calculated. Once the process notices a decrease in the training error and an increase in the validation error, learning stops automatically.

Input and output normalization

At the start of the process, the data was normalized to speed up learning and leads to faster convergence [35]. This normalization helps to establish a balanced scale, simplifying the artificial neural network by converting a complex high-dimensional predictive model into a simpler low-dimensional problem (Table 4). To achieve this normalization on input and output parameters, the following equation was employed [36]:

$$X^{norm} = \frac{\left(Y_{max} - Y_{min}\right)\left(X^{act} - X_{min}\right)}{\left(X_{max} - X_{min}\right)} + Y_{min} \tag{10}$$

In this equation, X^{act} represents the actual input/output value, while X^{norm} corresponds to

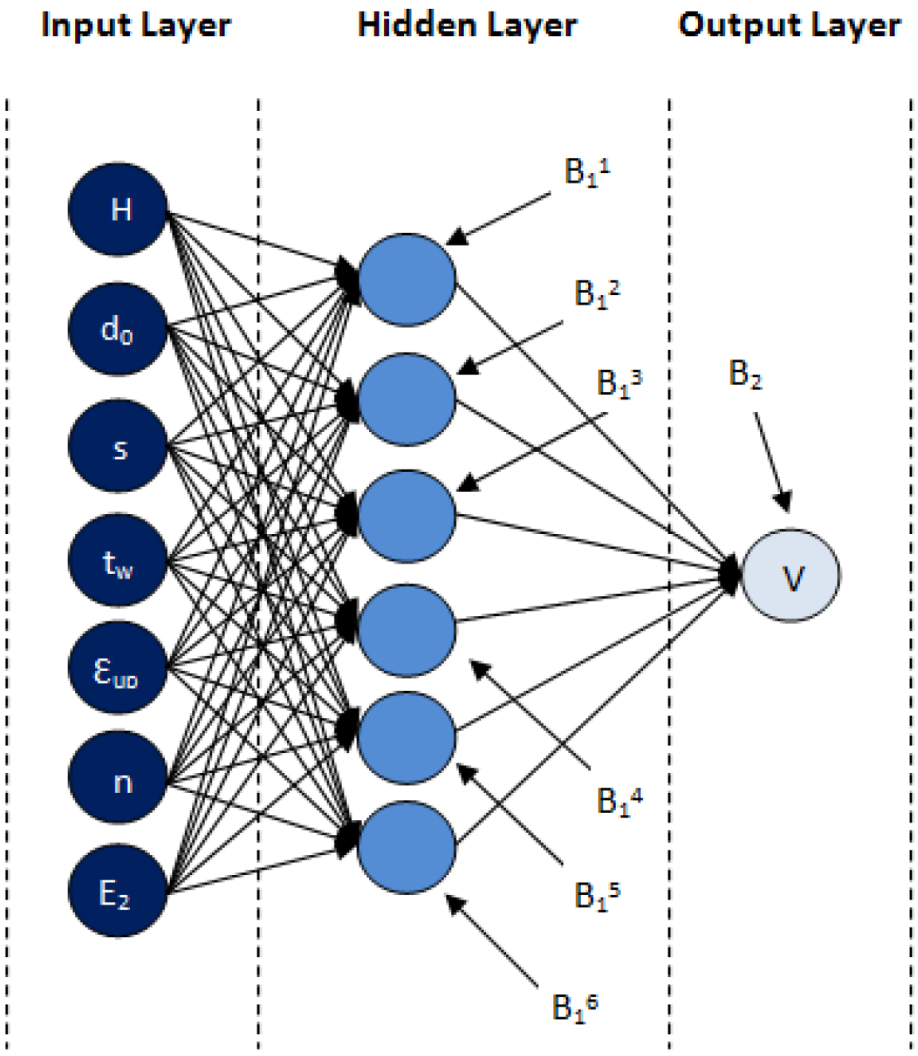

Figure 4. ANN Model with 3 neurons in the hidden layer

the normalized value. The term X_{max} denote the maximum values of the input/output parameters and X_{min} represent the minimum values of the input/output parameters. Y_{min} is the minimum value associated with each row of X (default, -1), and Y_{max} is the maximum value for each row of X (default, +1).

DECISION TREE

The decision tree is one of the machine learning methods characterized by its simplicity of interpretation, visualization of results and comprehension. Compared to other machine learning algorithms, data pre-processing for

Table 4. Parameters used to normalize input and target values

Input	X_{max}	X_{min}	Y_{min}	Y_{max}
H	1015.37	208.27	-1	1
d_0	762.96	121.92	-1	1
s	1068.14	134.11	-1	1
t_w	18.4	4.5	-1	1
ε_{up}	0.53	0.46	-1	1
n	10.19	7.35	-1	1
E_2	16581.71	13413.14	-1	1

regression trees is less demanding and does not require data normalization. This algorithm is a non-parametric static model for predicting complex relationships between input variables and an output variable. These regression trees are particularly advantageous when there is a non-linear relationship between the input parameters and the target variable. The program used in this study is Jupyter Notebook [37], which is an essential tool for Machine Learning with Python, users can code interactively while visualizing the results step by step. Thanks to its user-friendly environment, it facilitates data exploration, model building, and process documentation. The regression tree method works primarily by dividing the data set into smaller subgroups, then fitting a simple constant for each observation in each subgroup. However, this approach can sometimes be over-fitted, with lower predictive accuracy than more complex and sophisticated regression models.

For this study, we first developed a decision tree model that accurately predicts the shear strength of stainless steel cellular beams. Typically, two data sets are used in predictive modelling: a training set and a validation set. These sets are used to determine and evaluate the generalisability of the model. The training set is used to create and adjust the initial model, while the validation set is used to evaluate the overall performance and optimize the selected model [38]. In this case, 75% of the data has been allocated to training and 25% to validation, which means that 75% of the data will be used to modify the model, while the remaining 25% will be used to optimise it and improve its generalisation.

RANDOM FOREST ALGORITHM

Applied in Jupyter Notebook [37], Random Forest is a potent machine learning method extensively embraced in many domains. Among the ensemble learning techniques, this one combines several decision trees to raise prediction accuracy. While avoiding over-fitting, Random Forest stands out in particular for its capacity to manage vast, complicated data sets.

The Random Forest Regression (RFR) modelling technique is one of the most important mathematical tools in the field of machine learning. This approach aims to model the relationships between output variables and inputs, and is mainly based on the concept of decision trees (Breiman, 2001) [39]. Throughout the RFR modelling process, a large number of decision trees are developed and evaluated. Figure 8 schematically illustrates the regression diagram (RF).

When implementing the RFR, the variation in the number of trees was explored by adjusting the values to 100, 200, 300, 400 and 500. At the same time, the percentage of random training data was kept constant at 75%, while the proportion reserved for the test sample was maintained at 25%.

PERFORMANCE EVALUATION

To ensure accurate evaluation of results, a comparison between target and predicted values is essential. For this purpose, the regression value (R^2), mean absolute error (MAE) and root mean square error (RMSE) are calculated using Equations 11, 12 and 13 respectively. In these equations, t_i and O_i denote the actual and predicted resistance of the cellular beam web, respectively. The parameter N represents the overall number of data points contained in each set.

$$R^2 = 1 - \left(\frac{\sum_{i=1}^{N}(O_i - t_i)^2}{\sum_{i=1}^{N}(O_i)^2}\right) \tag{11}$$

$$MAE = \frac{1}{N}\sum_{i=1}^{N}\left|O_i - t_i\right| \tag{12}$$

$$RMSE = \sqrt{\frac{\sum_{i=1}^{N}\left(O_i - t_i\right)^2}{N}} \tag{13}$$

RESULTS AND DISCUSSION

Tables 5 and 7 show the R^2 values obtained using the ANN method during the different phases: training, validation and testing. Tables 6 and 8, on the other hand, shows all the results for regression values (R^2), RMSE and MAE for the entire data set. From the results obtained, we can clearly see that there is a clear relationship between improving the accuracy of the model and increasing the number of neurons. Figures 5 and 6 illustrate the difference between actual and predicted values for models with a single hidden layer with

Table 5. Regression values for training, validation and testing data sets

Input parameters	No. of Neurons	R^2		
		Training	Validation	Testing
H, d_0, s, t_w, ε_{up}, n, E_2	2	0.9906	0.99199	0.99227
	4	0.99766	0.99682	0.99776
	6	0.99837	0.99794	0.99821
	8	0.99823	0.99866	0.99787
	10	0.99798	0.99828	0.99745
	12	0.99875	0.99871	0.99702

Table 6. Output of ANN models for all data

Input parameters	No. of Neurons	All		
		R^2	MAE	RMSE
H, d_0, s, t_w, ε_{up}, n, E_2	2	0.9911	26.81	38.72
	4	0.99759	13.59	20.21
	6	0.99819	11.02	17.63
	8	0.99823	11.19	17.29
	10	0.99794	11.82	18.66
	12	0.99854	9.89	15.77

Table 7. Regression values for training, validation and testing data sets

Input parameters	No. of Neurons in the first Hidden Layer	No. of Neurons in the first Hidden Layer	R^2		
			Training	Validation	Testing
H, d_0, s, t_w, ε_{up}, n, E_2	4	4	0.99811	0.99823	0.99495
	4	8	0.9984	0.99843	0.99755
	4	12	0.99902	0.99877	0.99861
	8	4	0.99779	0.99835	0.99766
	8	8	0.99928	0.99882	0.9991
	8	12	0.99937	0.99887	0.99913
	12	4	0.99852	0.99727	0.998
	12	8	0.9985	0.99786	0.99805
	12	12	0.9991	0.9977	0.99711

Table 8. Output of ANN models

Input parameters	No. of Neurons in the first Hidden Layer	No. of Neurons in the first Hidden Layer	All		
			R^2	MAE	RMSE
H, d_0, s, t_w, ε_{up}, n, E_2	4	4	0.99762	12.72	20.14
	4	8	0.99828	11.71	17.03
	4	12	0.99891	9.72	13.57
	8	4	0.99785	12.19	19.04
	8	8	0.99919	8.69	11.70
	8	12	0.99925	8.07	11.28
	12	4	0.9983	10.80	16.94
	12	8	0.99831	10.96	16.88
	12	12	0.9986	10.09	15.41

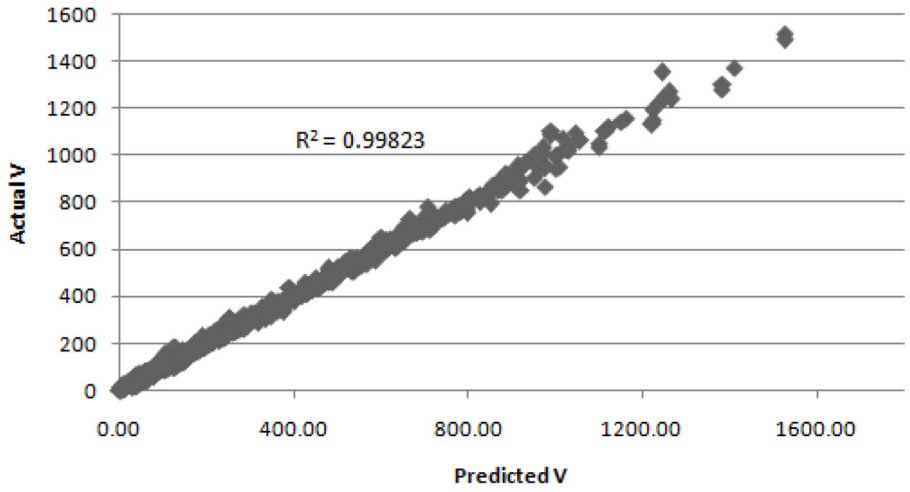

Figure 5. Actual vs predicted shear buckling model with a single hidden layer with 8 neurons

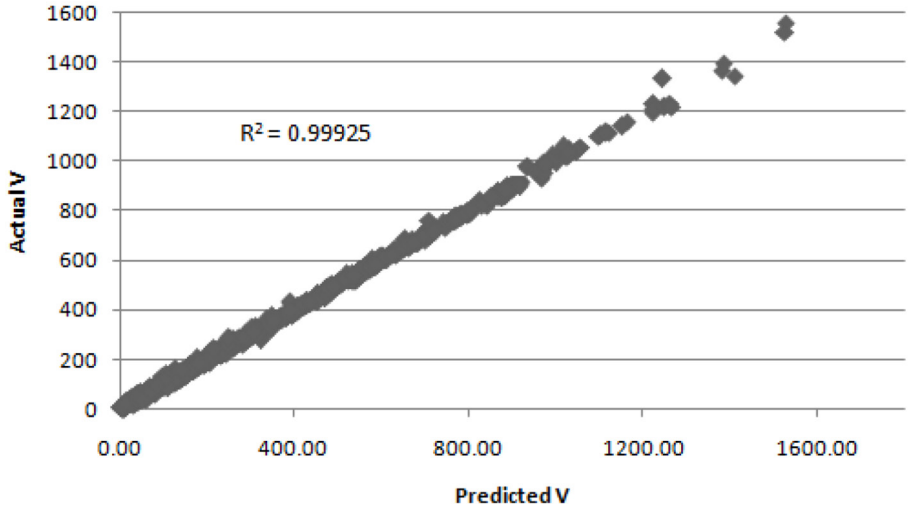

Figure 6. Actual vs predicted shear buckling model with two hidden layers with 8 and 12 neurons

8 neurons and two hidden layers with 8 and 12 neurons respectively.

The results shown in Table 8 clearly reveal that ANN models with 2 hidden layers generate more accurate predictions than ANN models relying exclusively on a single hidden layer. This increase in either the number of neurons or the number of hidden layers can also lead to overly complex models that are prone to overfitting. To circumvent this problem and simplify the resulting equations, it is preferable to use a model with a single hidden layer made up of 8 neurons, rather than a two-hidden-layer model with 8 and 12 neurons respectively in each layer. Indeed, the overall R^2, MAE and RMSE values for the case of a model with a single hidden layer composed of 8 neurons and a model with two hidden layers with 8 and 12 neurons respectively were 0.99823, 11.19 and 17.29 and 0.99925, 8.07 and 11.28 respectively. These figures indicate that, despite the improvement in accuracy, the single hidden layer model with 8 neurons retains remarkable precision and has the ability to predict with high accuracy the shear strength of the web of a stainless steel cellular beam. Although the performance of the two hidden layers model was higher than that of the single hidden layer model, we chose to work with an architecture comprising a single hidden layer and eight neurons. This choice will enable us to derive a formula characterized by its simplicity and practicality. Therefore, even though the two hidden layers model could reduce the RMSE and MAE, in this case it would lead to an increase in the number of model parameters. This would affect the practicality of the derived equation without providing a significant

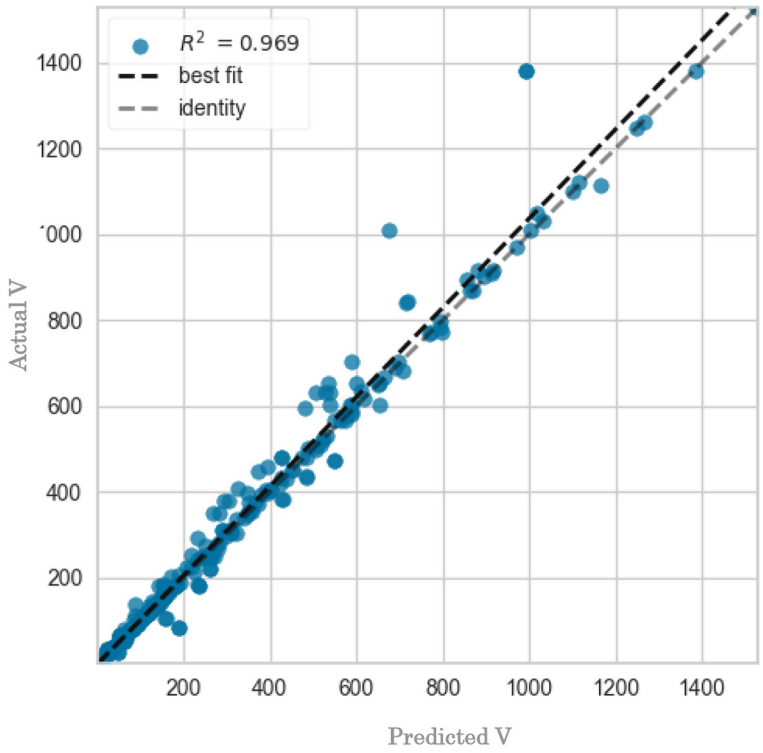

Figure 7. Actual vs predicted shear buckling model

improvement in accuracy for engineering applications, as the improvement in R^2 is 0.00102. In order to predict the shear strength of the web of a cellular beam with satisfactory accuracy, we carried out a comparison between the artificial neural network model, the Random Forest algorithm and the regression tree. The aim of this comparison is to determine the most accurate prediction method likely to deliver the most reliable results.

Figure 7 provides a detailed visualization of the differences between the actual values and the predicted values generated by the regression tree prediction method. This comparison demonstrates the model's ability to produce predictions that closely match real-world data. Figure 7 clearly shows the presicion of the regression tree method in estimating the shear strength of the web of cellular beams, with a remarkable R^2 value of 0.969. This regression value, which is close to 1, indicates a very good match between the model's predictions and the actual values. In other words, the model captures almost all the variability of the target variable, which means that it fits the data quite well. This high correlation between predicted and actual values indicates that the model successfully captures the complex relationships between the input variables, resulting in accurate predictions. This high accuracy highlights the capability of the regression tree approach as a powerful computational tool for structural analysis, making it an effective tool for estimating the shear strength of the web of cellular beams.

The results of the regression values (R2), RMSE and MAE obtained using the Random Forest algorithms are presented in Table 9. Figures 8 and 9 show the differences between the actual and predicted values for the 100 trees and 400 trees models, respectively. With a regression value (R^2) of 0.9909, a MAE of 9.87 and a RMSE of 15.98, the 400 trees model is particularly accurate. The reliability of the model is also confirmed by the high value of (R^2), indicating a very close match between predicted and actual values. The relatively low mean absolute error confirms that the model maintains a high level of accuracy in its estimates. In addition, the model's predictions generally remain close to the actual values when the mean square error is low, which ensures a high degree of predictive reliability. These results clearly demonstrate the Random Forest model's ability to reliably predict the shear strength of the web of a stainless steel cellular beam. The excellent correlation between the predicted and actual values confirms that the algorithm effectively captures the complexity of nonlinear relationships between the input variables and the output

Table 9. Output of RF models

Input parameters	No. of Tree	All		
		R^2	MAE	RMSE
H, d_0, s, t_w, ε_{up}, n, E_2	100	0.9839	11.51	16.17
	200	0.9877	10.43	16.58
	300	0.9885	10.64	17.57
	400	0.9909	9.87	15.98
	500	0.9862	10.73	18.54

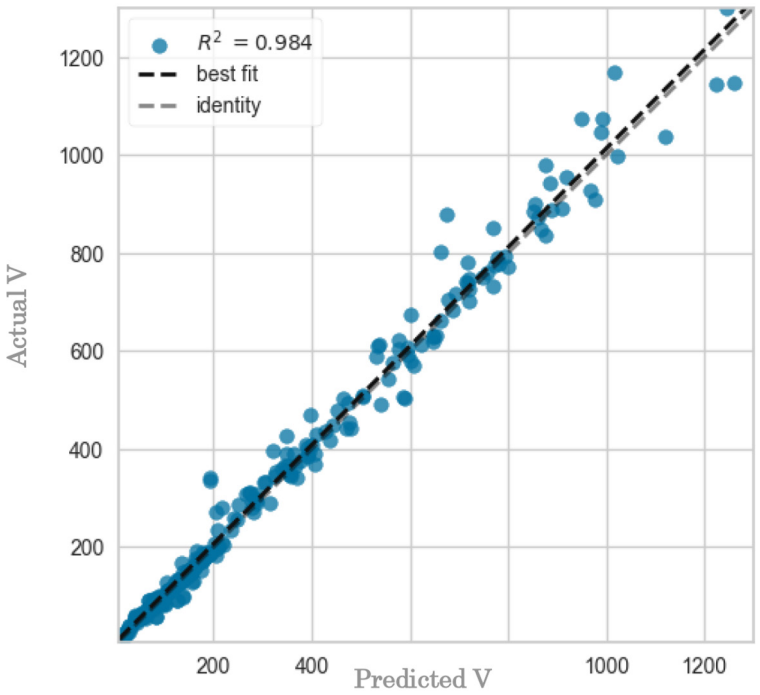

Figure 8. Actual vs predicted shear buckling model with 100 Tree

variable. It is important to note that the absence of clearly established evaluation standards makes the comparison of prediction methods complex. To solve this problem, we have chosen to compare the regression values (R^2) to determine the most accurate prediction method. Thus, by comparing the models with the highest prediction accuracy for each of the three machine learning methods used in this study.

Based on the conclusions drawn from the results, it is clear that all three models (artificial neural network, random forest algorithm and regression tree) manage to predict the shear strength of the web of cellular beams with satisfactory accuracy. These models reproduce the results obtained by numerical simulations with a high degree of precision. This conclusion is based on the high R^2 values and low errors obtained. The correspondence with the actual structural response is mainly due to the finite element model's ability to reproduce the physical mechanisms of web-post buckling, which has been previously verified both through experimental results for carbon steel and by applying appropriate constitutive laws for stainless steel.

Each model is capable of handling the input variables and producing predictions that closely match the observed values. However, a closer look at the regression R^2 values reveals significant differences in their performance. The artificial neural network (ANN) demonstrated superior predictive capability in the final comparison, as indicated by the R^2 values; however, additional operational criteria also support this choice. The ANN model offers a satisfactory compromise: it provides adequate prediction stability for deterministic finite element data and, above all, enables the derivation of an explicit design formula. On

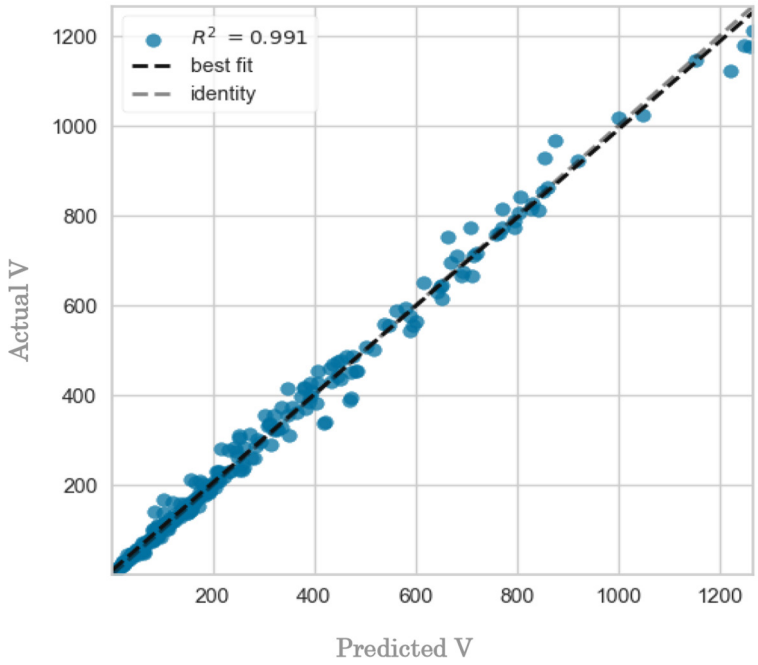

Figure 9. Actual vs predicted shear buckling model with 400 Tree

the other hand, Random Forest, although known for its robustness, produces a mathematical formula that is not as simple as that of the ANN model. As for decision trees, although simple, their accuracy is lower and their predictions show high variance. Of these models, the ANN-based machine learning approach produces the most accurate estimates, thanks to its ability to capture complex, non-linear relationships between input parameters and shear strength. This model is able to model complex patterns in the data that other algorithms might ignore, miss, or oversimplify. As a result, ANN has proven to be the most accurate and reliable method for predicting the shear strength of cellular beams. Equation 14 represents the formula developed from ANN to predict the normalized value of the web shear strength of cellular beams. It is essential to note that each input parameter must be normalized using Equation 10. To calculate the normalized shear resistance (V_n), the values H1, H2... H7 are calculated using Equation 15. In these equations, $(H)_n$, $(t_w)_n$, $(d_0)_n$, $(w)_n$ and $(R)_n$ represent the normalized values of the input parameters. The connection weights between the input neuron (i) and the hidden layer (j) are denoted by w_1 (i,j), while w_2 (i) denotes the connection weights between the hidden layer neurons (i) and the output, as shown in Table 10. B1 (i) corresponds to the bias for each neuron (i) in the hidden layer, and B_2 represents the output bias, which is equal to 0.82659. To determine the shear strength (V), a denormalization step is required.

Table 10. The connection weight and the bias values

Neuron	W_1(i,j)							W_2(i)	B_1(i)
	H	d_0	s	t_w	ε_{up}	n	E_2		
1	-0.8872	0.43096	0.7540	0.4527	1.0119	1.3043	-0.33935	0.41666	2.1528
2	1.5479	-1.5098	0.4128	0.4206	-0.0332	0.07150	0.060275	1.5641	-1.0419
3	0.69009	0.43065	-2.284	0.0290	-0.0632	0.09383	0.34533	0.4332	-1.1766
4	-0.8246	1.086	0.0922	1.2934	0.04561	-0.4152	-0.30601	-0.85517	-0.51318
5	0.54976	-0.1233	-1.2958	1.5125	-0.0731	0.04790	0.078179	0.23805	0.43588
6	1.105	1.5679	-0.4200	-2.3961	0.61449	0.06093	-0.06579	-0.92944	2.652
7	1.1032	-0.9870	-1.0338	-1.2608	-0.1034	0.61093	0.4689	-0.53928	0.55799
8	-0.1111	1.8119	-3.3077	0.8255	0.00622	0.28638	0.29219	-0.66658	-0.86229

From Equations 14 and 15, we can understand the effect of the geometric and mechanical properties of the beam on its buckling resistance. To be more explicit, these equations determine the main parameters that affect the behaviour of the web of cellular beams with regard to buckling. These parameters can be classified into two groups.

The first group consists of the parameters H, s, t_w, E_2, ε_{up} and n, which have a positive contribution to buckling resistance. That is, when these parameters increase, the beam becomes more rigid, which delays the onset of buckling and increases its resistance.

The second group includes the opening diameter, which has the opposite effect. Larger openings reduce the effective bearing area of the web, decrease stiffness and, consequently, weaken the web-post's resistance to buckling.

$$(V)_n = B_2 + \sum_{i=1}^{n=8} \omega_2(i)\left(\frac{2}{1+e^{-2H_i}} - 1\right) \quad (14)$$

$$H_i = B_1(i) + \omega_1(i,\,1)(H)_n + \omega_1(i,\,2)(d_0)n + \\ + \omega_1(i,\,3)(\mathrm{s})n + \omega_1(i,4)(t_w)n + \omega_1(i,\,5)(\varepsilon_{up})N + \\ + \omega_1(i,\,6)(n)n + \omega_1(i,\,7)(E_2)n \quad (15)$$

The robustness of the proposed ANN model was assessed not only based on its predictive accuracy but also on other criteria. Firstly, high performance on the training, validation and test datasets, with R^2 values above 0.99, confirms the model's generalization ability. Secondly, when modifying the number of neurons in the hidden layer, slight variations in the model's performance are observed, confirming its stability and robustness. However, despite the excellent predictive accuracy of the ANN model, its reliability is limited to the domain covered by the training database. Outside these limits, extrapolation is not recommended, as the model's behavior may be unpredictable in untrained domains. The final formula is therefore valid as long as the input parameters used are within the ranges shown in Table 4. It is advisable to avoid using this formula outside these ranges in order to maintain the reliability of the results obtained. Therefore, it is essential to ensure and verify that the geometric parameters of the beam and the material properties of the steel used comply with the prescribed limits. Based on these elements, we can confirm that the proposed approach is characterized by its accuracy and robustness within its defined field of application.

To facilitate the use of the ANN model, an Excel spreadsheet has been created. The user simply enters the input parameters (within the limits of Table 4) to instantly obtain the predicted strength.

CONCLUSIONS

The main objective of this study is to accurately predict the ultimate strength and develop a reliable design method for evaluating the web-post buckling of stainless steel cellular beams, and then to develop an equation for accurately calculating the web-post buckling resistance as a function of independent geometric parameters. From the analysis carried out and the results obtained, we can conclude that:

The artificial neural network was able to predict the shear strength of the web of cellular stainless steel beams more accurately than the Random Forest algorithm and the regression tree.

The ANN model with eight neurons showed very accurate predictions for the web-post buckling resistance. It also showed that the influence of the beams' geometric characteristics on their resistance was consistent with our expectations.

The use of an isolated web-post allows the buckling behavior of this web section to be studied. The proposed ANN model can determine the ultimate shear strength of the most stressed web-post within a beam. It is clear that load distribution is influenced by the interaction between the different web-posts in a cellular beam, but this does not alter the fact that using a single web-post model leads to conservative predictions in terms of design safety.

In general, an increase in the number of neurons in the hidden layer was found to be correlated with an improvement in the accuracy level for each model. Similarly for the Random Forest algorithm, increasing the number of trees leads to an increase in model accuracy.

The use of the ANN algorithm, created using the Levenberg-Marquardt backpropagation algorithm, has proved to be an effective means of accurately predicting the web-post buckling of stainless steel cellular beams. The resulting formula has considerable potential as a tool for accurately estimating the web-post buckling of stainless steel cellular beams.

This study establishes a reliable and robust methodology for determining and predicting the web-post buckling strength of stainless steel

cellular beams. Based on numerical simulations and using artificial neural networks, the final formula proposed represents a reliable and practical design tool. As a necessary extension of this work, it is recommended that future experimental studies be conducted on stainless steel cellular beams in order to provide definitive validation of the predictive models. These tests provide an experimental reference for finite element models, confirm the reliability of the proposed formula under real conditions, and obtain sufficient data to improve and recalibrate the models.

REFERENCES

1. Cashell K.A. et al. Experimental and numerical analysis of stainless steel cellular beams in fire, Fire Safety Journal 2021; 121: 103277.
2. Sheehan T,. Dai X., Lam D., Aggelopoulos E., Lawson M., Obiala R. Experimental study on long spanning composite cellular beam under flexure and shear. Journal of Constructional Steel Research 2016.
3. New Steel Construction. An introduction to cellular beams. New Steel Construction, http://www.newsteelconstruction.com/wp/an-introduction-to-cellular-beams/
4. Ellobody E., Nonlinear analysis of cellular steel beams under combined buckling modes, Thin-Walled Struct. 2012; 52: 66–79, http://dx.doi.org/10.1016/j.tws. 2011.12.009
5. El-Sawy K.M., Sweedan A.M.I., Martini M.I., Moment gradient factor of cellular steel beams under inelastic flexure, J. Constr. Steel Res. 2014; 98: 20–34, http://dx.doi.org/10.1016/j.jcsr.2014.02.007
6. Ferreira F.P.V., Rossi A., Martins C.H., Lateral–torsional buckling of cellular beams according to the possible updating of EC3, J. Constr. Steel Res. 2019; 153: 222–242, http://dx.doi.org/10.1016/j.jcsr.2018.10.011
7. Grilo L.F., Fakury R.H., de Souza Veríssimo G., Design procedure for the web-post buckling of steel cellular beams, J. Constr. Steel Res. 2018; 148: 525–541.
8. Panedpojaman P., Thepchatri T., Limkatanyu S., Novel design equations for shear strength of local web-post buckling in cellular beams, Thin-Walled Struct. 2014; 76: 92–104, http://dx.doi.org/10.1016/j.tws.2013.11.007
9. Shamass R., Guarracino F., Numerical and analytical analyses of high-strength steel cellular beams: A discerning approach, J. Constr. Steel Res. 2020; 166: 105911, http://dx.doi.org/10.1016/j.jcsr.2019.105911
10. Shamass R., Ferreira F.P.V., Limbachiya V., Santos L.F.P., Tsavdaridis K.D., Web-post buckling prediction resistance of steel beams with elliptically-based web openings using Artificial Neural Networks (ANN), Thin-Walled Structures. 2022; 180: 109959.
11. Lawson R.M., Lim J., Hicks S.J., Simms W.I., Design of composite asymmetric cellular beams and beams with large web openings, J. Constr. Steel Res. 2006; 62(6): 614–629.
12. Carvalho A.S., Rossi A., da R. Almeida M.M., Ozkılıç Y.O., Martins C.H., Artificial neural network modeling of the stability behavior of stainless steel I-beams with sinusoidal web openings, Engineering Structures 2024; 304: 117579.
13. Sharifi Y., Moghbeli A., Hosseinpour M., Sharifi H., Neural networks for lateral torsional buckling strength assessment of cellular steam I-beams, Adv. Struct. Eng. 2019; 22(3): 136943321983617.
14. Sharifi Y., Moghbeli A., Hosseinpour M., Sharifi H., Study of neural network models for the ultimate capacities of cellular steel beams, Iran. J. Sci. Technol. Trans. Civil Eng. 2019; 44: 579–589.
15. Limbachiya V., Shamass R., Application of Artificial Neural Networks for web-post shear resistance of cellular steel beams, Thin-Walled Struct. 2021; 161: 107414
16. Nguyen P.-C., Tran T.-T., Nguyen H.-P., Tran T.-D. Nonlinear Inelastic Local Buckling Behavior of Steel Columns Subjected to Axial Compression. Civil Engineering Journal, 2025; 11(9): 3916–3933. https://doi.org/10.28991/CEJ-2025-011-09-022
17. Ma Q., Li Y., Xiong K., Meng C., Zhou J. Seismic response analysis of buckling-restrained brace frames considering brace performance degradation. *Civil Engineering Journal*, 2025; 11(9): 3713–3731. https://doi.org/10.28991/CEJ-2025-011-09-09
18. Lopes N., Couto C., Vila Real P., Camotim D., Gonçalves R. Fire design of stainless steel I beams prone to lateral torsional buckling under end moments. Fire Saf J 2022; 131: 103609. https://doi.org/10.1016/j.firesaf.2022.103609
19. Shu G., Yang S., Jin X., Dong S., Jiang Q., Zheng B. Study on the bearing capacity of S600E high-strength stainless steel welded cross-sections. J Constr Steel Res 2020; 175: 106386. https://doi.org/10.1016/j.jcsr.2020.106386
20. Rossi, B.B. Discussion on the use of stainless steel in constructions in view of sustainability, Thin Walled Structures, 2014; 83: 182–189.
21. Topuz B., Çakici Alp N., Machine learning in architecture, Automation in Construction 2023; 154105012.
22. Adeli H., Yeh C. Perceptron learning in engineering design. Comput-Aided Civ Infrastruct Eng 1989; 4: 247–56.
23. Kifumbi F.M., Ngoma G.D., Erchiqui F., Tshibangu

T.M. Experimental and numerical modeling of a cross-flow turbine runner made of HDPE: Experimental and numerical approach. HighTech and Innovation Journal, 2025; 6(4): 1104–1122. https://doi.org/10.28991/HIJ-2025-06-04-01

24. Tsavdaridis K.D., D'Mello C., Web buckling study of the behaviour and strength of perforated steel beams with different novel web opening shapes, J. Constr. Steel Res. 2011; 67(10): 1605–1620.
25. Ward J., Design of Composite and Non-composite Cellular Beams, The Steel Construction Institute, SCI Publication, 1990; 100.
26. Rasmussen K.J. Full-range stress–strain curves for stainless steel alloys. Journal of constructional steel research 2003; 59(1): 47–61.
27. Hosseinpour M., Sharifi Y., Sharifi H., Neural network application for distortional buckling capacity assessment of castellated steel beams, Structures 2020; 27: 1174–1183.
28. Gholizaadeh S., Pirmoz A., Attarnejab R., Assessment of load carrying capacity of castellated steel beams by neural networks, J. Constr. Steel Res. 2011; 67(5): 770–779.
29. Kamane S.K., Patil N.K., Patagundi B.R., Use of artificial neural networks to predict the bending behaviour of steel I beam externally attached with FRP sheets, Mater. Today: Proceed. 2020 (in press).
30. Hedayat A.A., Afzadi E.A., Kalantaripour H., Morshedi E., Iranpour A., A new predictive model for the minimum strength requirement of steel moment frames using artificial neural network, Soil Dynam. Earthq. Eng. 2019; 116: 69–81.
31. MATLAB and Statistics Toolbox Release 2019a, The MathWorks, Inc., Natick, Massachusetts, United States, 2019.
32. Hosseinpour M., Sharifi Y., Sharifi H., Neural network application for distortional buckling capacity assessment of castellated steel beams, Structures 2020; 27: 1174–1183.
33. Abambres M., Rajana K., Tsavdaridis K.M., Ribeiro T.P., Neural network-based formula for the buckling load prediction of I-section cellular steel beams, Computers 2018; 8(1): 1–26.
34. Gupta T., Patel K.A., Siddique S., Sharma R.K., Chaudhary S., Prediction of mechanical properties of rubberised concrete exposed to elevated temperature using ANN, Measurement, 2019; 147: 106870.
35. Moradi M.J., Khaleghi M., Salimi J., Farhangi V., Ramezanianpour A.M., Predicting the compressive strength of concrete containing metakaolin with different properties using ANN, Measurement 2021; 183: 109790, http://dx.doi.org/10. 1016/j.measurement.2021.109790
36. Jin J., Li M., Jin L., Data normalization to accelerate training for linear neural net to predict tropical cyclone tracks, Math. Probl. Eng. 2015; 2015: 1–8, http://dx.doi.org/10.1155/2015/931629
37. Kluyver T., Ragan-kelley B., P´erez F., Granger B., Bussonnier M., Frederic J., Kelley K., Hamrick J., Grout J., Corlay S., Ivanov P., Avila D., Abdalla S., Willing C., Jupyter Notebooks—a publishing format for reproducible computational workflows. Position. Power Acad. Publ. 2016. https://doi.org/10.3233/ 978-1-61499-649-1-87
38. Gifford M., Bayrak T., A predictive analytics model for forecasting outcomes in the National Football League games using decision tree and logistic regression, Decision Analytics Journal 2023; 8: 100296.
39. Breiman L. Random Forests. Machine Learning 2001; 45: 5–32. https://doi.org/10.1023/A:1010933404324